CFD analysis of hydrodynamic force on a horizontal axis tidal turbine

Kai Xu, William Finnegan, Fergal O'Rourke and Jamie Goggins

Abstract—**Horizontal axis tidal turbines are similar to wind turbines in both geometry and principle of operation, yet they need to withstand much heavier loadings and extreme conditions in a harsh operating environment. Consequently, the loadings on tidal turbine blades need to be accurately evaluated within the design stage to ensure they can withstand loadings with little need for repair. With the advancement of computational capabilities, computational fluid dynamics offers a relatively inexpensive method of simulating working conditions and estimating loadings, compared to traditional physical testing, while maintaining accuracy and applicability under a range of operating conditions. In this research, a computational fluid dynamics model of a tidal turbine rotor has been developed using commercial code ANSYS CFX, where the three-dimensional blade geometry is developed from the prototype tidal turbine used in the Round Robin Tests in the framework of the H2020 MaRINET2 Infrastructures Network project. The outputs from the numerical model are validated against the experimental results, where it is revealed that with an increasing rotating speed of the tidal turbine, the thrust force that turbine experienced increases, while the torque force experiences a rise firstly, reaching a maximum value and then decreases gradually. In addition, the experimental results show that during the operation of ocean tidal turbines, the turbine blades experience frequent and large-scale fluctuation of hydrodynamic loads, including thrust and torque, which may lead to tidal turbine blade damage due to fatigue. Therefore, the next stage of development with this numerical model is fatigue loading evaluation, in order to improve the present fatigue design and testing of tidal turbine blades, while gaining a greater understanding of the damage mechanisms.**

Keywords—**Computational Fluid Dynamics, Fatigue, Turbine blades, Tidal energy.**

I. INTRODUCTION

Tidal energy convertor technology is expected to develop rapidly during the next decades considering the number of projects in progress and the obtained fundings in the last few years. Compared with other renewable energy sources, tidal energy has enormous potential with numerous highly energetic sites worldwide and the advantages as it is predictable over large timescales [1]. According to an EU report by Corsatea and Magagna [2], 76% of research and development in the tidal sector are related to horizontal axis tidal turbines. Horizontal axis tidal turbine's rotor axis is parallel to the incoming water flow and is similar to wind turbines from a concept and design point of view. Because the density of water is much larger than air, tidal turbines need to withstand much heavier loadings and extreme conditions in a harsh operating environment under water.

Recently, inter-laboratory tests, referred as Round Robin Tests (RRTs) in the framework of EC-Funded R&D project H2020 MaRINET2 and former successful MaRINET Infrastructures Networks project, have been undertaken with similar testing facilities and under same testing conditions to identify the influence of test environments on the device's performance [3], [4]. In that programme, the exact same 0.724m diameter horizontal axis tidal turbine is tested in three tanks, i.e., the wave and current flume tank of IFREMER, the towing tank of CNRINM and FLOWAVE circular combined wave and current tank, where the turbine performance is measured and the impact of testing turbines towed in calm water or fixed in an onset flow with non-negligible turbulence levels is investigated.

In recent years, Computational Fluid Dynamics (CFD) is gaining popularity because of its advantages in high accuracy and versatility under different a range of

©2023 European Wave and Tidal Energy Conference. This paper has been subjected to single-blind peer review.

Sponsor and financial support acknowledgement: This research was funded in part by Science Foundation Ireland (SFI) through the MaREI Research Centre for Energy, Climate and Marine (Grant no. 12/RC/2302_2) and the European Commission through the H2020 CRIMSON project (grant agreement no.: 971209).

K. Xu is with the Department of Civil Engineering, MaREI Centre, Ryan Institute, University of Galway, Galway, Ireland (e-mail: k.xu1@nuigalway.ie).

W. Finnegan is with the Department of Civil Engineering, MaREI Centre, Ryan Institute, University of Galway, Galway, Ireland (e-mail: william.finnegan@nuigalway.ie).

F. O'Rourke is with the Centre for Energy and Renewables at Dundalk Institute of Technology, Dundalk, County Louth, Ireland (e-mail: fergal.orourke@dkit.ie).

J. Goggins is with the Department of Civil Engineering, MaREI Centre, Ryan Institute, University of Galway, Galway, Ireland (e-mail: william.finnegan@nuigalway.ie).

Digital Object Identifier: https://doi.org/10.36688/ewtec-2023-137

operating conditions with increasing computational capacities. Many commercial codes such as ANSY CFX and ANSY Fluent are widely used in present simulations of tidal turbines. The aim of this paper is to investigate the hydrodynamic force on a horizontal axis tidal turbine using Computational Fluid Dynamics. To achieve this aim, the following objectives are completed in this study:

- To develop a numerical model of a tidal turbine rotor using ANSYS CFX, where the three-dimensional blade geometry is developed from the prototype tidal turbine used in the Round Robin Tests of the H2020 MaRINET2 project,
- To validate the numerical outcomes of hydrodynamic force including thrust and torque with the experimental results from the MaRINET2 datasets and improve the accuracy of numerical results by meshing refinement and setup adjustment,
- Compare the experimental results of MaRINET2 datasets and discuss the fatigue issue causing from the fluctuations of hydrodynamic force on turbine to find out the direction for the next stage of the modelling.

TABLE I
NOMENCLATURE

Symbol	Quantity	Unit
A	Rotor Area	m²
C_P	Power coefficient	
C_T	Thrust coefficient	
k	Turbulence kinetic energy	m²/s²
p	Thermodynamic pressure	Pa
p'	Modified pressure	Pa
Q	Rotor toque	N·m
R	Blade tip radius	m
S_M	Sum of body forces	N
t	Time	s
T	Rotor thrust	N
TSR	Tip speed ratio	
U_c	Velocity of current	m/s
U_i, U_j, U_k	Vector of velocity	m/s
x_i, x_j, x_k	Spatial distances	m
μ	Laminar viscosity	Pa·s
μ_{eff}	Effective viscosity	Pa·s
μ_t	Turbulent viscosity	Pa·s
ρ	Fluid denstiy	kg/m³
ω	Rotational speed of rotor	rad/s

II. THEORY

A. Governing Equations –CFD Solver

Reynolds-averaged Navier-Stokes equations of momentum and mass conservation is used in the ANSYS CFX solver to approximately simulate the flow field conditions around a tidal current turbine [5], [6]. The continuity equation as shown in (1) and the momentum conservation equation as shown in (2) are solved together.

$$\frac{\partial \rho}{\partial t} + \frac{\partial}{\partial x_j}\left(\rho U_j\right) = 0 \tag{1}$$

$$\frac{\partial (\rho U_i)}{\partial t} + \frac{\partial (\rho U_i U_j)}{\partial x_j} = -\frac{\partial p'}{\partial x_i} + \frac{\partial}{\partial x_j}\left[\mu_{eff}\left(\frac{\partial U_i}{\partial x_j} + \frac{\partial U_j}{\partial x_i}\right)\right] + S_M \tag{2}$$

where ρ is the fluid density, U_i and U_j are the velocities of the flow averaged over time t, x_i and x_j are the spatial distance, S_M is the sum of body forces, μ_{eff} is the effective viscosity which is determined using (3) and p' is modified pressure as defined in (4).

$$\mu_{eff} = \mu + \mu_t \tag{3}$$

$$p' = p + \frac{2}{3}\rho k + \frac{2}{3}\mu_{eff}\frac{\partial U_k}{\partial x_k} \tag{4}$$

where μ is the laminar viscosity, μ_t is the turbulence viscosity, p is the thermodynamic pressure, k is the turbulence kinetic energy and U_k and x_k are the velocity and spatial distance in their respective planar dimensions.

The Shear Stress Transport (SST) model was chosen, as it is a combination of k-ω model near walls and the standard k-ε model away from walls using a blending function, utilizing the advantages of both models to model flow separation as well as account for the shear stress transport in adverse pressure gradient boundary layers [7].

ANSYS CFX provides General Grid Interface (GGI) feature, where a connection across a GGI attachment or periodic condition can be performed using the control surface approach. The physically based intersection GGI algorithm is employed to provide the complete freedom to change the grid topology and physical distribution across the interface, constructing connecting interface successfully between the overlapping regions of the two sides of the interface, even for mismatched surfaces. CFX solver also features Multiple Frames of Reference (MFR) based on the GGI technology, focusing on the investigation of rotor/stator interaction for rotating machinery. These features were utilized in this work for the benefits of reducing the complexity of the numerical model. [6].

B. Non- dimensional Coefficients

The hydrodynamic forces on tidal turbine rotors including thrust and torque force are investigated in this study, where the numerical results are validated by the experimental outcome from MaRINET2 project dataset [8]. During the comparison, the non-dimensional coefficients, i.e., Thrust Coefficient (C_T), Power Coefficient (C_P) and Tip Speed Ratio (TSR) can be obtained in the following way [9]:

Tip Speed Ratio: $$\mathrm{TSR} = \frac{\omega R}{U_c} \tag{5}$$

Power coefficient: $$C_P = \frac{Q\omega R}{(1/2)\rho {U_c}^3 A} \quad (6)$$

Thrust coefficient: $$C_T = \frac{T}{(1/2)\rho {U_c}^2 A} \quad (7)$$

where ω is the rotational speed of rotor, R and A are the blade tip radius and rotor area, U_c is the current velocity, Q and T are the rotor torque and thrust.

III. METHODOLOGY

C. Turbine Blade Geometry Creation

In the Round Robin Tests (RRTs) in the MaRINET2 project, the turbine blades are modelled using the NACA 63-418 profile (see[10] for profile details). A more detailed geometrical description of the blade with the chord, pitch and thickness distribution is shown in Table II. A summary description of the testing structure is presented in Table III [3].

TABLE II
DETAILED BLADE GEOMETRICAL DESCRIPTION WITH THE CHORD (c), THE PITCH ANGLE AND THE THICKNESS (t) IN FUNCTION OF THE VARYING RADIUS r [3].

r/R	c/R	Pitch (deg)	t/c (%)
0.1333	0.0567	29.5672	80.0
0.1500	0.0567	29.5672	100.0
0.1550	0.0567	29.5672	100.0
0.1983	0.1521	25.6273	36.0
0.2417	0.2474	22.1491	21.3
0.2850	0.2375	19.3031	21.4
0.3283	0.2259	16.9737	21.7
0.3717	0.2141	15.0538	22.0
0.4150	0.2029	13.4572	22.2
0.4583	0.1925	12.1169	22.4
0.5017	0.1829	10.9815	22.5
0.5450	0.1743	10.0114	22.5
0.5883	0.1665	9.1761	22.4
0.6317	0.1594	8.4516	22.2
0.6750	0.1529	7.8191	21.9
0.7183	0.1471	7.2638	21.5
0.7617	0.1418	6.7735	20.9
0.8050	0.1370	6.3387	20.2
0.8483	0.1325	5.9514	19.5
0.8917	0.1285	5.6050	18.6
0.9350	0.1247	5.2941	18.0
0.9783	0.1213	5.0143	18.0
1.0000	0.0655	4.8743	25.0

TABLE III
GENERAL DESCRIPTION OF THE TESTING TURBINE MODEL [3].

Profile	NACA 63418
Rotor radius (R)	350 mm
Hub radius	46 mm
Hub length	720 mm
Studied TSR	[0 – 7]
Sense of rotation	Counter-clockwise
Reynolds (Re_∞)	[140 – 420] x 10^3

In this research, a three-dimensional blade rotor geometry is developed from the prototype tidal turbine used in the Round Robin Tests in MaRINET2 project, as previously detailed. The profile sections were generated using the NACA Airfoil Generator which can be found in [11].

All 23 sections created were exported in .txt file format an then they were imported into the 3D solid geometry modeller (SolidWorks). With the loft feature, the solid geometry of the horizontal axis tidal turbine blade rotor was generated, and it was imported into ANSYS Workbench afterwards.

D. Mesh and flow setting

The following setup was made in this ANSYS CFX research. To improve the computational efficiency, one third of the turbine was used in the numerical simulation and the domains were angled at 120° .

The computational domain was separated into stationary and rotating domain, which was connected using the GGI feature. In consideration of the radius of the tidal turbine is approximately 0.362 m, the large stator domain extended 1 m, 2 m and 1 m in the upstream, downstream and radial direction respectively. The rotating domain extended 0.37 m in the radial direction with a thickness of around 0.11 m.

The mesh was setup in the stationary domain with a maximum element size of 0.2 m and a face meshing size of 0.01m in the interface between stationary and rotating domain. The maximum element size defined in the rotating domain was 0.02 m. Mesh inflation has been specified at the surface of the tidal turbine, with 5 layers of a growth rate 1.2 and a maximum thickness of 0.1 m. These refinements to the mesh result in an overall mesh size of approximately 2.5 million elements (or 0.63 million nodes), as shown in Fig. 1 and Fig. 2.

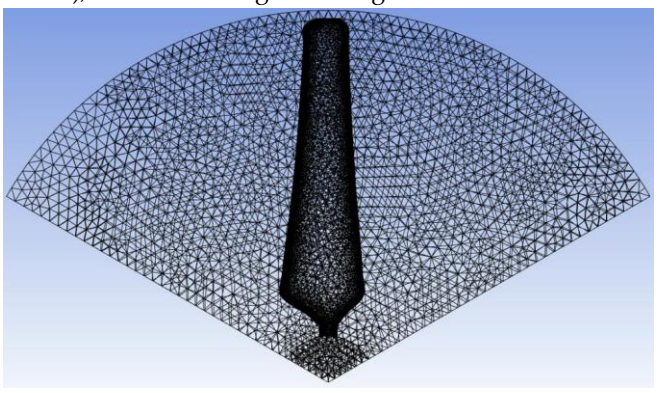

Fig. 1. Mesh generated at 2,487,334 elements and 788,072 nodes in rotating domain.

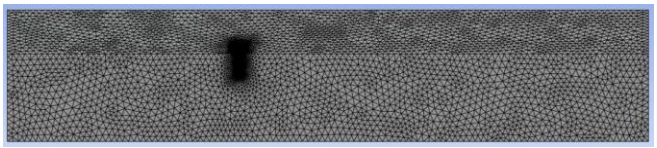

Fig. 2. Mesh generated at 247,794 elements and 48,189 nodes in stationary domain.

The k-ω shear stress transport (SST) turbulence model was chosen for this study. The angular velocity was set at a series of rotating speeds performed in the experimental tests in MaRINET2 project for the rotating domain. The surface of the blade was set to "no slip wall" and was assumed to be "smooth wall". As both the stationary and the rotating domains are fluid domains, their interfaces were set up using the "fluid-fluid" interface type. Because the large outer domain is stationary while the smaller inner fluid domain has a rotating frame of reference, the "frozen rotor" option was chosen.

The upstream inlet current speed was set with 1 m/s, the same as which is used in the MaRINET2 tests, with the turbulence option of "Medium (Intensity = 5%)". The downstream outlet boundary type was set as "Outlet".

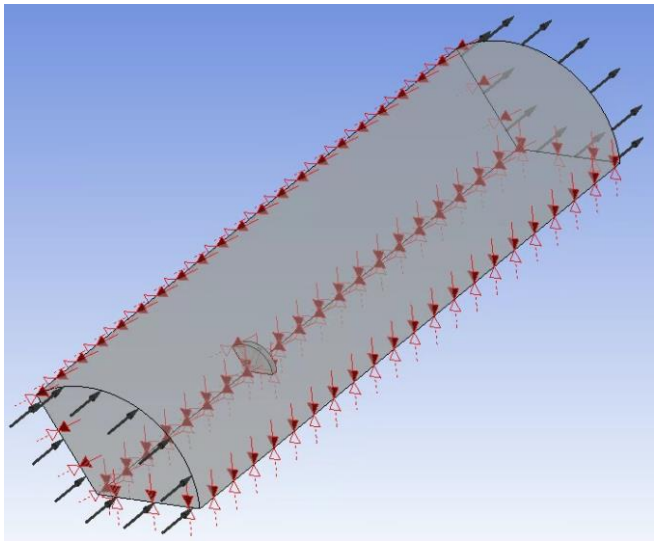

Fig. 3. Preview of CFX setup

IV. Results and Discussion

The numerical results of hydrodynamic forces including thrust and torque force on the tidal turbine rotor along with the experimental outcome from MaRINET2 dataset [8] are shown in Fig. 4 and 5. The numerical and experimental results share the same trend

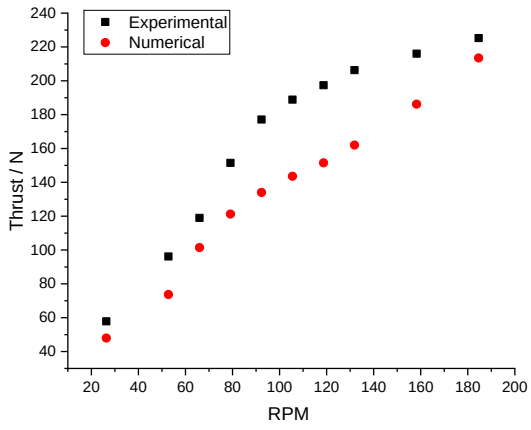

Fig. 4. Variation of experimental and numerical outcomes of thrust force on turbine rotor in only current (U_c = 1m/s) with different turbine rotating speeds.

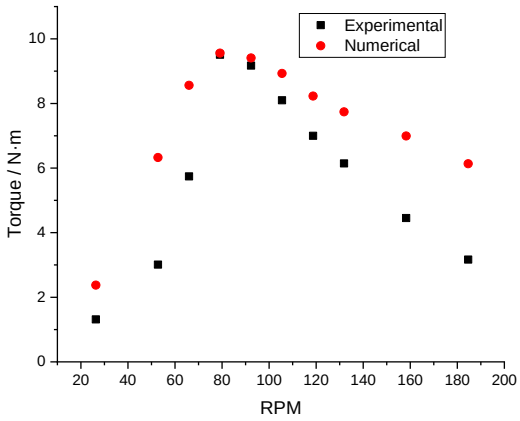

Fig. 5. Variation of experimental and numerical outcomes of torque force on turbine rotor in only current (U_c = 1m/s) with different turbine rotating speeds.

while there are notable deviations between numerical and experimental results, for thrust force the average deviation is around 19% and for toque force the average deviation is around 45%.

A mesh independence study was performed to compare the convergence of numerical results with increased number of element and nodes by decreasing element size, as shown in Table IV. Table IV was tabulated to show the significance of different meshing element size in the results and the computational time taken for each to converge for the same RMS residual target 0.00002 for a rotating speed of 184.65 RPM, which is the maximum rotational speed of rotor in MaRINET2 tests, as well as averaged deviations in the series of tests compared with experimental results. The study was performed using a Dell Latitude 5420 Laptop housing an 11th Gen Intel® Core™ i7-1165G7 CPU @2.80GHz 1.69 GHz with a 32.0 GB RAM setup. The 'Microsoft MPI Local Parallel' run mode option with 7 partitions within the ANSYS-CFX Solver Manager was chosen.

TABLE IV
MESH INDEPENDENCE STUDY OF THE CONVERGENCE OF NUMERICAL RESULTS.

Mesh	1	2	3
Element Size (m)	0.01	0.007	0.005
Number of Nodes	584,378	794,836	1,052,130
Number of Elements	2,261,374	3,170,408	4,349,050
T (N) for 184.65 RPM	213.50	206.69	215.87
ΔT (%) for 184.65 RPM		-3.19	1.11
Average ΔT (%) to Experimental Results	19	19	18
Q (N·m) for 184.65 RPM	6.13	5.59	6.57
ΔQ (%) for 184.65 RPM		-8.81	7.18
Average ΔQ (%) to Experimental Results	45	45	48
Computational Time for 184.65 RPM	2 hours 6 minutes	2 hours 24 minutes	5 hours 19 minutes

The experimental result obtained for the rotating speed of 184.65 RPM in terms of thrust force was 225.25 N and torque force was 3.1675 N·m. For the mesh independence study, compared with 584,378 nodes in the mesh,

1,052,130 nodes provided results with similar accuracy and took over twice the time to run. Considering the meshing of 794,836, the study provided smaller thrust and torque force for the rotating speed of 184.65 RPM, yet the overall deviation for the whole series of testing, the averaged deviation was still similar.

A mesh refinement study was performed to improve the numerical models and narrow the gap between numerical and experimental results, including increasing inflation layers along the turbine surface, decreasing the inflation growth rate, increasing element number by introducing face meshing on the blade surface, in order to improve meshing quality by adding more nodes around the interface between the turbine and fluid, as shown in Table V. Table V was tabulated to show the significance of different meshing refinement in the averaged deviations between numerical and experimental results and it reveals that the former mentioned changes made little improvement to results, while inducing the setup of a first layer height of 0.000277m with Y+ insensitive near wall treatment did help, reducing the deviation of torque force to around 39%, as shown in Fig. 6 and Fig. 7.

TABLE V
MESH REFINEMENT STUDY OF NUMERICAL RESULTS.

Mesh Refinement Method	Number of Nodes	Number of Elements	ΔT (%)	ΔQ (%)
Inflation 7*1	619,081	2,073,224	19	46
Inflation growth rate 1.15	922,172	794,836	19	45
Inflation Y+ 0.000277 m	788,072	2,487,334	20	39
Face element size 0.005 m	794,403	2,504,095	20	40
Face element size 0.0007 m	1,871,285	5,148,396	20	39
Face meshing Method	788,513	2,490,354	20	38

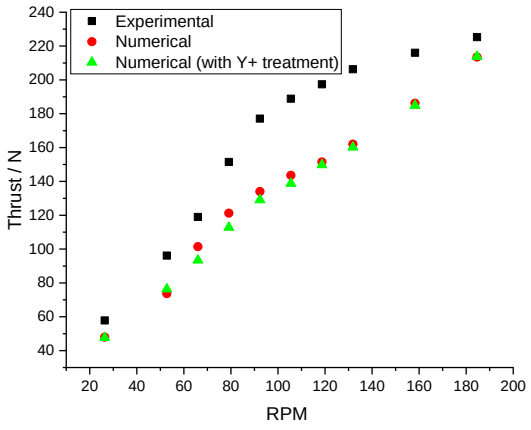

Fig. 6. Comparison of experimental and improved numerical outcomes of thrust force on turbine rotor in only current (U_c = 1m/s) with different turbine rotating speeds.

A non-dimensional analysis of numerical results compared with experimental outcome of MaRINET2 dataset [8] has also been conducted, using the non-dimensional parameter of Thrust Coefficient (C_T), Power

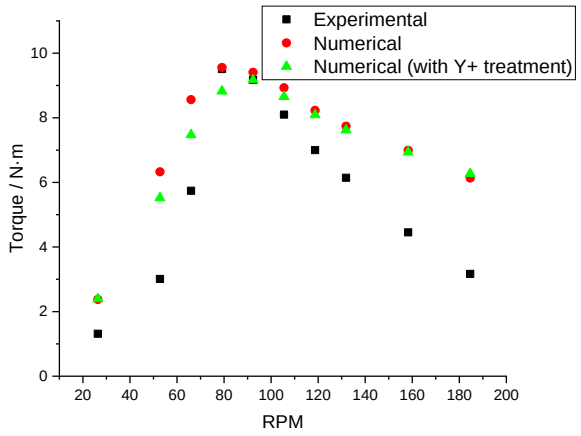

Fig. 7. Comparison of experimental and improved numerical outcomes of torque force on turbine rotor in only current (U_c = 1m/s) with different turbine rotating speeds.

Coefficient (C_P) and Tip Speed Ratio (TSR), as shown in Fig. 8 and Fig. 9. In the former mentioned cases of a rotating domain thickness of 0.11m, for the thrust coefficient, the numerical results increase similarly compared to experimental ones, while for toque

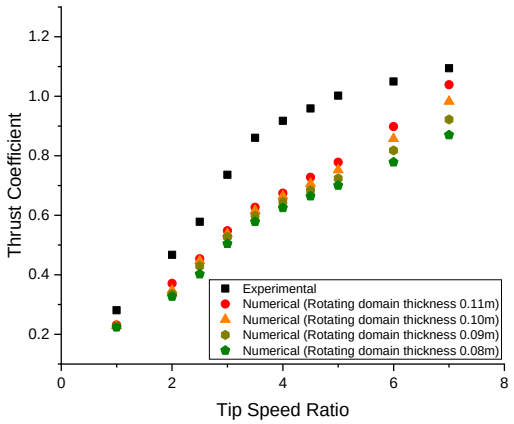

Fig. 8. Variation of experimental and numerical outcomes of thrust coefficient on turbine rotor in only current (U_c = 1m/s) with different Tip Speed Ratios.

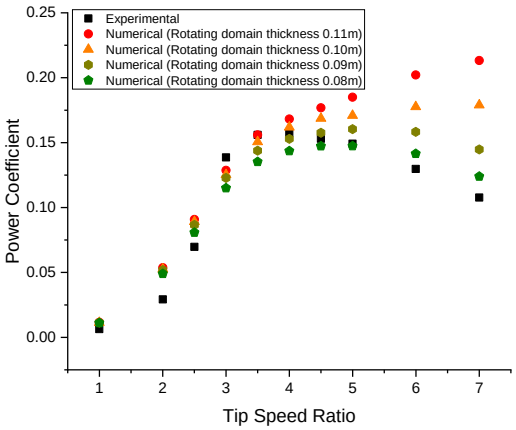

Fig. 9. Variation of experimental and numerical outcomes of torque coefficient on turbine rotor in only current (U_c = 1m/s) with different Tip Speed Ratios.

coefficient, the numerical and experimental outcome increases with the increase of tip speed ratio until TSR reaches 3.5, then there exists a notable difference, the experimental C_P results decrease with increase of TSR, yet the numerical C_P results increase with increase of TSR with a much smaller increasing trend. To locate the cause of this difference, a series of investigations have been conducted, as a result, it is found that reducing the thickness of rotating domain while maintaining the diameter of rotating domain unchanged has an influence. As the volume of rotating domain decreases, the power coefficient and thrust coefficient decreases, and the trend of the power coefficient turns similar to the experimental outcome. Because the rotation of rotating domain is used to represent the rotation of turbine, it proves that it is important to choose the size of rotating domain carefully.

E. Fatigue

In the dataset of the MaRINET2 project [8], the result of a series of flume tests in current and wave conditions is also given. The thrust force of rotor and blade in test "run003" and "run054" at IFREMER within one wave circulation is illustrated in Fig. 10 and Fig. 11 [12]. To explain, the frequency of wave is 0.6Hz and the experimental sampling frequency is 128Hz, so around 213 data is used to demonstrate the force variation in one circulation of wave. As can be seen in Fig. 10, the fluctuation turns much bigger after the addition of wave, from round 3% of the mean thrust to 28%. It is noted that for a tidal turbine of 42 RPM, 1.67 secs could contain over one rotations of turbine blades, yet the huge fluctuation of thrust in one turbine blade is still meaningful as illustrated in Fig. 11. This shows that the fluctuation of thrust loading on turbine blades is even larger, and it is essential to combine fatigue into the design of tidal turbine blades.

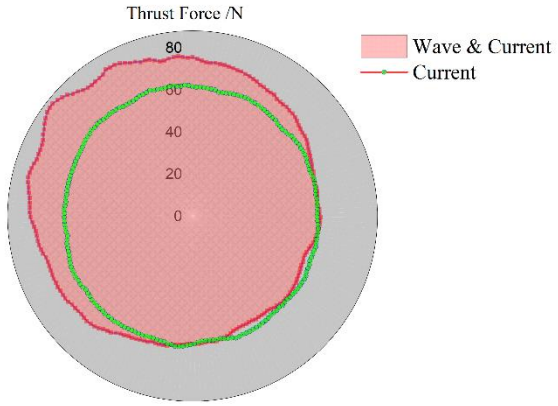

Fig. 10. Variation of thrust force on tidal turbine rotor in only current (U_c = 0.8m/s, turbulence 1.5%) and current/ wave conditions (0.155m amplitude, 0.6Hz frequency) within one wave period.

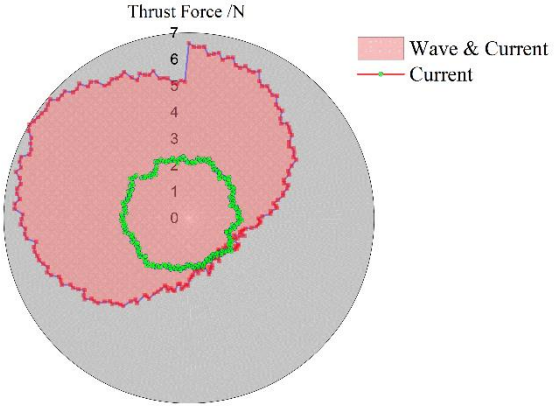

Fig. 11. Variation of thrust force on one blade of tidal turbine in only current (U_c = 0.8m/s, turbulence 1.5%) and current/ wave conditions (0.155m amplitude, 0.6Hz frequency) within one wave period.

V. CONCLUSION

The numerical results are validated with the experimental dataset of MaRINET2 Project, and meshing refinement has been conducted to narrow the averaged deviations between the numerical and experimental outcome, reaching 20% for thrust force and 40% for torque force. The results reveal that with the increasing of the rotating speed of the tidal turbine, the thrust force that turbine experienced increases rapidly until the rotating speed reaches 80 RPM and then the increase rate reduces, while the torque force experiences a rise firstly, reaching a maximum value and then decreases gradually. When it comes to the non-dimensional thrust coefficient and power coefficient, the changing trends with tip speed ratio are similar. The experimental results show that during the operation of ocean tidal turbines, the turbine blades experience frequent and large-scale fluctuation of hydrodynamic loads, including thrust and torque, especially when the surface wave plays a role in the performance of turbines. This inevitable and significant fluctuation will lead to serious tidal turbine blade fatigue problems even damage, and it is essential to combine fatigue into the design of tidal turbine blades.

VI. FUTURE WORK

Systematic numerical investigations on tidal turbines will be conducted in our research. A more extensive mesh refinement study will be carried out to narrow the present deviations between numerical and experimental results and achieve greater accuracy as well as mesh quality. In addition, the next stage of our research is the evaluation of fluctuations of hydrodynamic loadings on tidal turbines, in order to improve the present fatigue design and testing of tidal turbine blades. However, to achieve this aim, the following objectives will be completed as well:

- To build a wave tank model and research on the fluctuation of hydrodynamic force including thrust and torque on tidal turbines under wave and current conditions,
- To experimentally study on turbine performance in the wave tank at University of Galway to gain a greater understanding of the damage mechanisms of tidal turbines blades due to fatigue.

REFERENCES

[1] Green Match, "Tidal Energy and Wind Power in the UK | GreenMatch," Jul. 2017. https://www.greenmatch.co.uk/blog/2016/10/tidal-and-wind-energy-in-the-uk (accessed Apr. 11, 2023).

[2] T. D. Corsatea and Davide Magagna, "Overview of European innovation activities in marine energy technology | Policy Commons," *JRC Science and Policy Reports*, 2013, Accessed: Apr. 11, 2023. [Online]. Available: https://policycommons.net/artifacts/2163587/overview-of-european-innovation-activities-in-marine-energy-technology/2919100/

[3] B. Gaurier *et al.*, "Tidal energy 'round Robin' tests comparisons between towing tank and circulating tank results," *International Journal of Marine Energy*, vol. 12, pp. 87–109, Dec. 2015, doi: 10.1016/j.ijome.2015.05.005.

[4] B. Gaurier *et al.*, "MaRINET2 tidal energy round robin tests-performance comparison of a horizontal axis turbine subjected to combined wave and current conditions," *J Mar Sci Eng*, vol. 8, no. 6, Jun. 2020, doi: 10.3390/JMSE8060463.

[5] W. M. J. Batten, M. E. Harrison, and A. S. Bahaj, "Accuracy of the actuator disc-RANS approach for predicting the performance and wake of tidal turbines," *Philosophical Transactions of the Royal Society A: Mathematical, Physical and Engineering Sciences*, vol. 371, no. 1985, 2013, doi: 10.1098/rsta.2012.0293.

[6] "Ansys CFX-Solver Theory Guide," 2021. https://dl.cfdexperts.net/cfd_resources/Ansys_Documentation/CFX/Ansys_CFX-Solver_Theory_Guide.pdf (accessed Apr. 14, 2023).

[7] F. R. Menter, "Zonal two equation κ-ω turbulence models for aerodynamic flows," *AIAA 23rd Fluid Dynamics, Plasmadynamics, and Lasers Conference, 1993*, 1993, doi: 10.2514/6.1993-2906.

[8] Gaurier Benoit *et al.*, "MaRINET2 Tidal 'Round Robin' dataset: comparisons between towing and circulating tanks test results for a tidal energy converter submitted to wave and current interactions," *SEANOE*, 2021. https://www.seanoe.org/data/00471/58265/ (accessed May 10, 2023).

[9] A. S. Bahaj, A. F. Molland, J. R. Chaplin, and W. M. J. Batten, "Power and thrust measurements of marine current turbines under various hydrodynamic flow conditions in a cavitation tunnel and a towing tank," *Renew Energy*, vol. 32, no. 3, pp. 407–426, Mar. 2007, doi: 10.1016/j.renene.2006.01.012.

[10] "Theory of Wing Sections: Including a Summary of Airfoil Data - Ira H. Abbott, A. E. von Doenhoff - Google Books." https://books.google.com.hk/books?hl=en&lr=&id=lWe8AQAAQBAJ&oi=fnd&pg=PT7&dq=I.H.+Abbott,+A.E.+Von+Doenhoff,+Theory+of+Wing+Sections,+Including+a+Summary+of+Airfoil+Data,+Dover+Books+on+AeronauticalEngineering+Series,+Dover+Publications+Inc.,+1959&ots=H1T9tBmDGC&sig=KkSKnyvvJ8e9v3WD5wVIgEkUBgs&redir_esc=y#v=onepage&q&f=false (accessed Apr. 19, 2023).

[11] "NACA Airfoil Generator.," Jan. 2019. https://github.com/adeharo9/NACA-airfoil-generator (accessed Apr. 20, 2023).

[12] Kai Xu, William Finnegan, Fergal O'Rourke, and Jamie Goggins, "Hydrodynamic modelling of marine tidal turbines: A state of the art review," in *Civil Engineering Research in Ireland Conference (CERI 2022)*, 2022, pp. 520–524.